Remediation of 4-Nitroaniline by Plaster-Based Permeable Reactive Barriers Containing Zero Valent Iron (ZVI): Precast Plaster Retaining Wall Blocks for Environmental Applications

saliha boudia
Universite Mouloud Mammeri de Tizi Ouzou
farida fernane
Universite Mouloud Mammeri de Tizi Ouzou
patrick j sharrock
Université Toulouse III Paul Sabatier: Universite Toulouse III Paul Sabatier
marina m.l. fiallo (marina.fiallo@iut-tlse3.fr)
Université Toulouse III Paul Sabatier: Universite Toulouse III Paul Sabatier https://orcid.org/0000-0001-7704-9388

Research Article

Keywords: groundwater remediation, zero-valent iron, nitroaniline, pollutants, plaster, precast retaining wall block

Posted Date: March 15th, 2021

DOI: https://doi.org/10.21203/rs.3.rs-281415/v1

Remediation of 4-nitroaniline by plaster-based permeable reactive barriers containing zero valent iron (ZVI): precast plaster retaining wall blocks for environmental applications

Saliha Boudia[a,b], Farida Fernane[a], Patrick Sharrock[b], Marina Fiallo[b]*,

[a]Mouloud Mammeri University , Natural Resources Laboratory, Tizi-Ouzou 15000 Algeria

[b]Chemistry department, IUT A, Université Toulouse 3 Paul Sabatier, 81104 Castres, France

*Corresponding author: marina.fiallo@iut-tlse3.fr, phone ++33(0)563621553

Keywords: groundwater remediation, zero-valent iron, nitroaniline, pollutants, plaster, precast retaining wall block

Graphical abstract

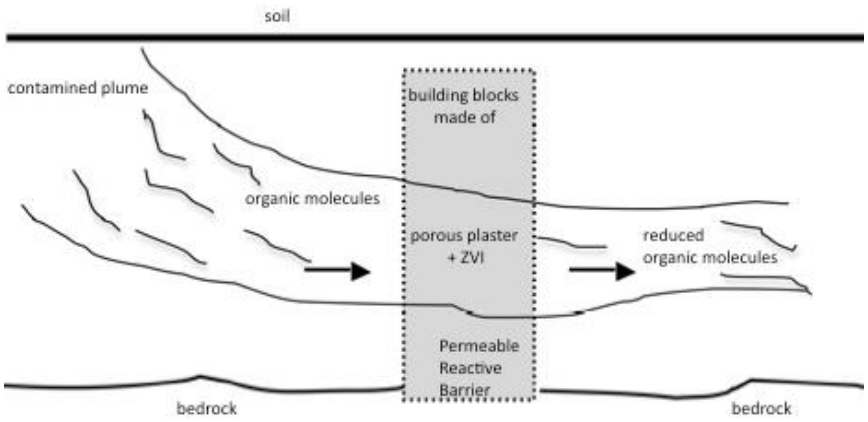

Highlights files

- Precast plaster blocks were tested for environmental applications

- Zero Valent Iron (ZVI) dispersed in plaster blocks was active in reducing 4-nitroaniline (PNA) to p-phenylenediammine with a reactive capacity of 55 mg/g (PNA/ZVI)

- Permeability of plaster blocks can be modulated depending on composite formulation.

Abbreviations: **PDA**, p-phenylenediamine; **PE**, polyethylene; **PET**, polyethylene terephtalate; **PNA**, 4-nitroaniline (or p-nitroaniline)

Abstract

Permeable reactive barrier (PRB) containing zero valent iron (ZVI), plaster and additives to make a porous composite structure was tested to remove an organic nitro compound as model pollutant. An aqueous solution of 4-nitroaniline (PNA) was passed through a porous plaster composite column and chemical degradation quantified by UV-Vis spectroscopy. PNA was reduced to p-phenylenediamine and the rate of the reduction was strongly related to ZVI amount, pollutant volume, and the contact rate with metal particles. The parameters could be controlled by reactor design and operation. The columns were made to test the materials for making precast plaster blocks containing ZVI. The results showed that such porous plaster blocks could be efficient as retaining walls for environmental applications.

1. Introduction

Permeable reactive barrier (PRB) is a cost-effective technology for “in situ passive method” of groundwater remediation (Henderson and Demond 2007). It is an implementation of filtration consisting in a permeable zone, which passively captures a plume of contaminants through immobilization or transformation of pollutants, releasing decontaminated water to the other side of the barrier (Grajales-Mesa and Malina 2016). PRB is generally composed of inexpensive filler materials, doped with specific reagents for remediation of unwanted compounds. It was reported that zero valent iron (ZVI) is particularly effective in chemical

44 degradation of persistent chlorinated compounds into non-toxic and harmless by-products
45 (Dorathi and Kandasamy 2012).
46 Nitrocompounds are usually present in hair dyes (Various authors 1992), in pharmaceuticals,
47 such as chloroamphenicol (Various authors 1989a) and metronidazole (Gavrilescu et al.
48 2015), and nitroarenes has been identified in vehicle exhausts (Various authors 1989).
49 Nitroarenes can be reduced to corresponding anilines, in presence of ZVI and hydrochloric
50 acid, in Bechamp reduction (Béchamp 1854); moreover, in organic synthesis other methods
51 have found to be more specific and to reduce by-pass products (Schabel et al. 2013). For
52 instance, silver nanoparticles were developed for in situ catalytic reduction method of PNA
53 (Farooqi et al. 2018). However, in order to integrate in PRB a low cost reactant, ZVI has
54 already shown to be a good candidate for reduction of different pollutants (Hu et al. 2018;
55 Eljamal et al. 2018, 2020; Khalil et al. 2018; Maamoun et al. 2018, 2020, 2020a). Efficiency
56 of PRB is related to flow of polluted plume and to pollutant characteristics (Wantanaphong et
57 al. 2006; Touze, et al. 2004).
58 Calcium sulfates (including plaster, $CaSO_4 \cdot 0.5H_2O$, and its dihydrated product, gypsum,
59 $CaSO_4 \cdot 2H_2O$) were chosen as inert substrate in order to prepare composites. They are low
60 cost building materials, sometime considered as a waste when by-product in industrial
61 preparation of phosphoric acid (Saadaoui et al. 2017). One great advantage of calcium
62 sulfates is that they are compatible with a variety of fillers, still retaining adequate
63 mechanical properties. The main problem in using them for geological applications is their
64 relative solubility, which, however, could be an advantage in an environmental approach: in
65 fact a calcium sulfate-based PRB should break up with time discharging in environment no
66 toxic species.
67 We researched the possibility of using plaster as barrier component for controlling liquid
68 flow rates while simultaneously introducing a low cost reactive material. Our aim was to

verify if plaster can be used for permeable barrier construction and if ZVI retains its redox properties when included in a solid shell.

A plaster-based composite, shaped as a column, was formulated in order to make a model barrier to study ZVI efficiency for soluble organic species depollution, such as 4-nitroaniline as pollutant model.

Key factors of all-in-one composites design for PRB were investigated as follows:

1- Permeability of solid plaster, as inert support for PRB, was determined and a method to improve it was developed (giving "porous" plaster)

2- "Porous" plaster was tested for its mechanical properties and the better formulation chosen.

3- ZVI was inserted in "porous" plaster and new composites were checked for their mechanical properties giving a formulation with a good compromise for all parameters.

4- Reduction of 4-nitroaniline was performed in batch with ZVI as in Béchamp reaction, in order to establish reaction chemical parameters (amount of reactive specie, pH values).

5- Degradation of 4-nitroaniline (PNA, used as model pollutant) to p-phenylenediamine (PPD), was quantified by UV spectroscopy by measuring its absorbance maximum at 380 nm.

5- Reduction of 4-nitroaniline was performed in column as a model for all-in-one PRB system: breakdown and exhaustion points were determined for specific experimental conditions.

2. Experimental

2.1. Chemicals

Plaster, in chemical form of $CaSO_4 \cdot 0.5H_2O$, was a commercial powder (plaster of Paris quality) from Parexlanko, France; iron powder (ZVI, 325 mesh, 99%), H_3PO_4 (85%), and

$CaCO_3$ (99%) were from Acros (France), 4-nitroaniline (or p-nitroaniline, PNA, 98%) and p-phenylendiamine (PDA, 98%) from Aldrich (France).

2.2. Material characterization

Solid samples were characterized by powder X-ray diffraction (XRD) with a Bruker D2 X'PertPRO diffractometer using Cu Kα radiation (40 kV and 40 mA). Crystallographic identification of $CaSO_4 \cdot 2H_2O$ was accomplished by comparing the experimental XRD pattern to COD 2300259 of gypsum standard (point group 2/m).

2.3. Physical and mechanics tests

All samples were weighted and "apparent" density calculated from geometrical parameters. Indirect tensile stress diametral compression tests were carried out with a Zwick Roll Z020 testing machine (Zwick Roell, France) at a crosshead speed of 10 mm/min, until failure. Using initial height (L [m]) and diameter (D [m^2]) of each sample, and measuring the reciprocated force (F [kg/ms^2]) from compression, indirect (or Brazilian) tensile strength, σ_T ([kg/m^2s^2]), was calculated from its definition in equation 1:

$$\sigma_T = \frac{2F}{\pi LD} \quad (1)$$

2.4. Porosity determination

Porosity was determined from the ratio of experimental "apparent" density of each sample and gypsum density, $CaSO_4 \cdot 2H_2O$, 2.308 g/cm^3 (CRC Handbook of Chemistry and Physics, 2019) with equation 2:

$$porosity(\%) = \frac{density_{exp}}{density_{gypsum}} \times 100 \quad (2)$$

2.5. Spectroscopic analysis

UV-VIS spectra were used to quantify 4-nitroaniline (PNA) and p-phenylendiamine (PDA) concentrations. Vis-UV spectra were recorded between 200 and 700 nm in aqueous solution on a HP 8453 spectrophotometer with quartz cells of 0.2 and 1 cm of path-length. Spectra of

pure 4-nitroaniline (PNA) and p-phenylendiamine (PDA) were recorded in aqueous solution giving the following spectroscopic features: PNA: 380 (ε=73.3 $L \cdot mol^{-1} cm^{-1}$), 227 (35.5), 204 (63.0) nm. PDA: 305 (ε=13.7 $L \cdot mol^{-1} cm^{-1}$), 240 (49.3), 210 (58.7) nm. PNA concentrations in solution were determined from absorbances measured at 380. PDA formation (following mechanism of Bechamp reduction) was checked from band at 240 nm (PDA maximum absorption).

2.6. Determination of PNA degradation

Degradation of PNA, meaning the disappearing of its characteristic absorption band at 380 nm), was calculated from the UV-Vis spectra with equation 3:

$$degradation(\%) = \frac{\left(A_{380} - A_{600}\right)}{\left(A^{\circ}_{380} - A^{\circ}_{600}\right)} \times 100 \qquad (3)$$

where A_{380} and A_{600} are the absorption values of each sample at the noted wavelengths, and $A°_{380}$ and $A°_{700}$ the absorption values of starting solutions. Absorption values were corrected at 600 nm in order to avoid diffusion effects from cloudy solutions. At 380 nm the absorption contribution for presence of PDA in aqueous solutions was insignificant.

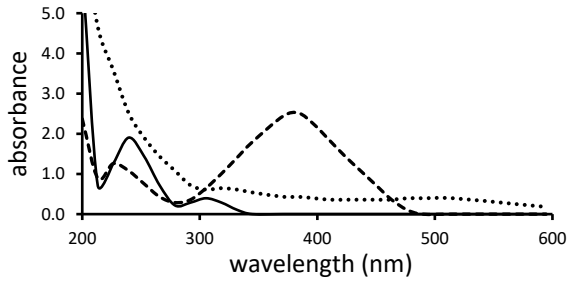

Figure 1 Absorption spectra of PNA (---), PDA (—) and PDA polymerization product (¨) in aqueous solutions: [PNA]= [PDA]= 30 mg/l; path-length quartz cell = 0.2 cm

2.7. Plaster samples preparation

139 Plaster slabs were made by adding plaster (50 g) to appropriate amounts of distilled water.
140 After 5 minutes of mixing, preparations were poured into PET (polyethylene terephtalate) or
141 PE (polyethylene) cylindrical molds to make samples for flow experiments (in 2.8-cm-
142 diameter, 2-cm-high) and for mechanical tests and density measurements (in 2.6-cm-
143 diameter, 5-cm-heigh). All solid samples were dried at 60°C for 24 hours before their use.

144 2.7.1. Effect of water

145 In these series of experiment the water/plaster ratio was modified, as reported in Table 1, and
146 physical and mechanical properties measured for each sample, giving the results reported in
147 Table 1.

Water/plaster ratio (w/w)	density (g/ml)	porosity (%)	indirect tensile strength (MPa)
0.5	1.15±0.04	50.46±0.40	7.14±0.43
0.6	1.10±0.04	52.71±0.33	5.47±0.41
0.7	1.04±0.06	55.06±0.61	4.48±0.43
0.8	0.99±0.05	57.39±2.00	3.57±0.19

148

149 **Table 1** Physical and mechanical properties of plaster samples (density, porosity, indirect
150 tensile strength) as a function of plaster/water ratio (w/w); experimental conditions: plaster
151 (50.00 g); measurements were an average from ten samples.

152 These sample were checked for their permeability (see section 2.7.5)

153 2.7.2. Effect of porogen ($CaCO_3$+H_3PO_4)

154 Porous samples were prepared by grinding calcium carbonate (pure or recovered from
155 calcined egg shell waste) with plaster powder, then pouring the powder in phosphoric acid–
156 containing water.

157 Permeability of these samples was compared with those of “compact” plaster (see section
158 2.7.5).

H_3PO_4 (g)	H_3PO_4 (%)	density (g/ml)	porosity (%)	indirect tensile strength (MPa)
0.00	0	1.04±0.06	55.06±0.61	4.48±0.43
0.34	0.3	0.86±0.06	63.08±2.72	1.48±0.09
0.68	0.6	0.76±0.01	66.97±0.35	1.15±0.73
1.01	0.8	0.74±0.03	67.94±2.62	1.04±0.25
1.35	1.1	0.72±0.01	69.13±1.80	0.83±0.08

Table 2 Physical and mechanical properties of plaster samples (density, porosity, indirect tensile strength) as a function of H_3PO_4 added; experimental conditions: plaster (50.0g, 41.6%); water (58.2 %); $CaCO_3$ (0.2%)

2.7.3. Effect of acid

The effect of mineral acid on plaster setting was tested with H_3PO_4 and HCl: if acidic solutions increased porosity compared to distilled water, however samples with hydrochloric acid were more dense and compact than those made with phosphoric acid (Table 3).

acid	density (g/ml)	porosity (%)	indirect tensile strength (MPa)
0	1.04±0.06	55.06±0.61	4.48±0.43
H_3PO_4	0.52±0.07	77.55±0.61	1.89±0.65
HCl	0.94±0.02	59.48±0.67	5.87±1.90

Table 3 Physical and mechanical properties of plaster samples (density, porosity, indirect tensile strength) as a function of H_3PO_4 added; experimental conditions: plaster (50.0g, 41.6%); water (58.2 %); $CaCO_3$ (0.2%)

2.7.4. Effect of ZVI

Different amounts of ZVI were dispersed in solid components (plaster and calcium carbonate) before adding liquid components (water and phosphoric acid), in order to uniformly scatter heavy iron in slab. Physical and mechanical properties of different samples obtained were reported in Table 4.

ZVI (g)	ZVI percentage (%)	density (g/ml)	porosity (%)	indirect tensile strength (kPa)
0	0	0.86±0.06	63.08±2.72	1.48±0.09
1.00	1.2	0.88±0.29	62.19±0.66	1.26±0.27
2.00	2.3	1.17±0.05	49.56±0.37	1.93±0.30
3.00	3.4	1.36±0.05	41.23±0.93	3.18±0.88
5.00	5.6	1.36±0.06	41.32±0.57	3.14±0.51

Table 4 Physical and mechanical properties of plaster samples (density, porosity, indirect tensile strength) as a function of ZVI added; experimental conditions: plaster (50.0 g, 41.0%); water (57.4%); $CaCO_3$ (0.2%); H_3PO_4 (0.2%)

2.7.5. Permeability coefficient measurements

Permeability coefficient measurements were done on plaster samples (2.8-cm diameter, 2.0-cm heigth) with a water pressure column of 5 cm. Discharge of water (Q [m^3/s]) percolating under a constant head difference (H [m]) through a sample, of porous material of cross area S ([m^2]) and length L ([m]), was determined for several samples as in Tables 5. Permeability coefficients K (hydraulic conductivity, [m/s]) were calculated from Darcy's law, following equation 4:

$$K = \frac{QL}{SH} \quad (4)$$

,

Serie	water/plaster (w/w)	$CaCO_3$+H_3PO_4 (%)	ZVI (%)	pH values	permeability coefficient (m/s)

1	0.7	-	-	7.1	$\geq 8.23 \cdot 10^{-8}$
2	0.7	0.4	-	7.4	$2.88 \pm 0.13 \cdot 10^{-5}$
3	0.7	-	2	7.1	$\geq 8.23 \cdot 10^{-8}$
4	0.7	0.4	2	7.3	2.24 ± 0.7410^{-5}

192

193 **Table 5** Permeability coefficients of plaster samples as a function of composition.
194 Experimental conditions: plaster (50.0 g, 41.0%); experiments were an average of five
195 samples.

196

197 For the samples containing "compact" plaster (series 1 and 3), discharge was very slow and
198 permeability coefficients were estimated from water amount recovered after 24 hours.

199 2.7.6. Column formulation

200 In a further step, only composites with a permeability allowing to study PRB chemical
201 reactivity in period of one day, were used in depolluting tests.

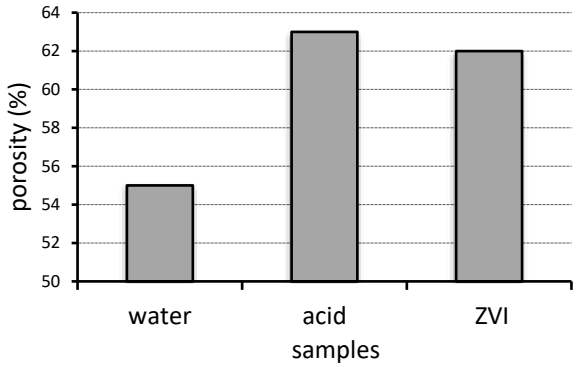

202

203 **Figure 2** Porosity optimization as a function of different components of BRP (water,
204 phosphoric acid and ZVI) plaster (50.0 g, 40.0%); water (56.0%); $CaCO_3$ (0.2%); H_3PO_4
205 (0.2%)

206

207 Figure 2 reported the optimization of all composite components (water, calcium carbonate,
208 phosphoric acid, ZVI) for a fixed amount of plaster in order to keep a good equilibrium

between different physical properties. Final composite formulation contained plaster and water with 0.7 ratio, 0.2% $CaCO_3$ and 0.4% H_3PO_4 (per 50 g of plaster), used to mold depolluting columns.

2.8. Bechamp reduction

2.8.1. ZVI in batch reaction

Batch experiments were conducted inside 250 ml Erlemeyer flasks under continuous magnetic stirring (500 rpm) and the overall time of experiments was 7 hours. Batch experimental initial conditions were: temperature; 25°C, PNA concentration; 30mg/l, water volume; 100 ml. Specific variables in batch experiments included pH (initial pH acidic or neutral) and the amounts of ZVI (1, 2 and 3 g). Sampling was conducted within accumulative time of 15 minutes during first three hours, then of 1 hour for last four from commencement of batch experiments, For analysis, 2 ml samples were withdrawn by a 5 ml syringe, Vis-UV spectra registered using a 1 cm quartz cell, then returned to batch. Initial pH was adjusted, or not, using 95% phosphoric acid.

In both experiments, degradation percentage was calculated from absorbance values at 380 nm corresponding maximum absorption of PNA, as indicated in Section 2.5.

2.8.2. Column preparation

100 g of plaster, mixed with appropriate amounts of ZVI and 0.2% $CaCO_3$, were added to 70 ml of distilled water, containing 0.4 g of phosphoric acid, then all reagents were mixed together and the viscous mixture poured into PET (polyethylene terephtalate) cylindrical molds (in 5.0-cm-diameter, 15-cm-heigh) used as percolator system. PET shells were thermally fixed to plaster columns in order to avoid leaking out from their extremities.

2.8.3. ZVI in column reaction

PNA-containing aqueous solutions (100 ml aliquots) were passed by percolation through columns. Fractions of 100 ml were recovered post-column: 2 ml of each fraction was checked

by UV-Vis spectrum between 200 and 700 nm and absorbance values at 380 nm (wavelength of maximum absorbance for PNA) used to calculate PNA concentration in each fraction, as indicated in Section 2.5.

2.9. SEM Analysis

Plaster samples were observed by scanning electron microscopy (SEM) Zeiss Supra 55VP.

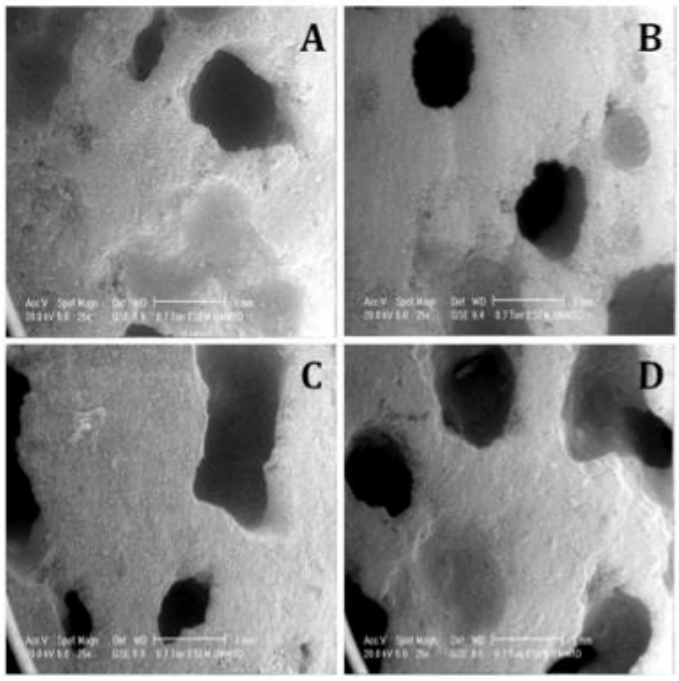

Figure 3 SEM photographs showing a view of porogen-containing hardened gypsum samples, prepared with a water-to-plaster ratio of 0.7, as a function of carbonate amounts (with 1.1 % phosphoric acid, w/w). $CaCO_3$: A=0.2%, B=0.5g, C=0.7g, D= 0.9% (w/w); length scale bar is 1mm and magnification x25)

2.10. Speciation of ZVI reacting species

Samples of plaster-based composites (2.8-cm diameter, 2.0-cm heigth) were soaked in distilled water (25 ml) and pH was measured as a function of time. O-phenathroline (0.5%) and KSCN (1%) in aqueous solution were used to check presence of Fe(II) or Fe(III) species,

respectively. Because of the low amount of iron species in solution, reagents were used in strong excess but quantification was not reliable.

3. Results and discussion

Calcium sulfates (including starting material, plaster, $CaSO_4 \cdot 0.5\ H_2O$, and its hydrated product, gypsum, $CaSO_4 \cdot 2H_2O$) were chosen as inert substrate in order to prepare porous composites. They are low cost materials, sometime considered as a waste as in the case of phosphogypsum (Chernysh et al. 2021) compatible with a variety of fillers, still retaining adequate mechanical properties. The main problem in using them for geological applications is their relative solubility, which could be an advantage for environmental approach: in fact a calcium sulfate-based PRB should break up with time discharging in environment only no toxic species.

Hemihydrate calcium phosphate ($CaSO_4 \cdot 0.5H_2O$), named plaster, became gypsum when hydrated ($CaSO_4 \cdot 2H_2O$); however plaster denomination was here extended to "hydrated samples", with no reference to their chemical state. Different formulations were prepared, by using plaster, water, chemical porogen and "reactive components" (ZVI) in different proportions. For each sample, density, porosity, permeability, and mechanical properties were determined.

3.1.1 Properties of plaster-based composites

It was reported that water amount determined porosity in plasters blocks (Lewry and Williamson 1994; Adrien et al. 2016); as reported in Table 1, density and indirect tensile strength of materials were reduced as a function of water contents and porosity increased.

In reaction between plaster ($CaSO_4 \cdot 0.5H_2O$) and water to form gypsum ($CaSO_4 \cdot 2H_2O$), part of water is consumed by hydration reaction during material setting and remainder slowly

275 evaporated leading to porosity (Diaga Seck et al. 2015); hardening of plaster paste leads to
276 porous structure, made of entangled needle-shape gypsum crystals (Jaffel et al. 2006).
277 However, in order to allow percolation in short times, porosity, as shown in Table 5, obtained
278 only by water evaporation was not enough to have an acceptable permeability and a better
279 porogen for plaster was sought.
280 Calcium carbonate was used as porogen in presence of acid in order to generate open porosity
281 and increase permeability through the column (Table 2); phosphoric acid was chosen because
282 eventual formation of calcium phosphate as secondary product was supposed to not modify
283 plaster structure: the two materials are perfectly compatible, moreover giving composites
284 with lower dissolution rates and enhanced mechanical properties (Fisher et al. 2012).
285 In presence of increasing amount of H_3PO_4, porosity increased when density and mechanical
286 properties decreased, in agreement with cavity formation following CO_2 degassing during
287 material setting (Table 2). Starting from 0.5% acid, porosity was not significantly modified,
288 as well as mechanical properties. However, permeability increased three times of magnitude
289 compared to "compact" plaster. Calcium phosphates, probably formed, was dispersed in
290 gypsum matrix with no effects on physical and mechanical parameters. It was reported that
291 weak acids (such as citric acid) play a role as plastifier, retarding setting (Lanzóna and
292 García-Ruiz 2012) because citric acid partially inhibits binder hydration from hemihydrate to
293 dihydrate.
294 Compatibility of $CaCO_3$ in plaster (up to 1.5 %) was checked in order to verify density and
295 porosity of composites. Moreover, if total porosity seemed little affected by increasing
296 amount of $CaCO_3$, pore dimensions were bigger (Figure 3). In SEM images of porogen-
297 containing samples in Figure 3, presence of 1 mm pores of diameter was evident.
298 A ^{1}H NMR relaxation study of water, confined in porous medium of hardening gypsum,
299 described coexistence of two water populations, in permeable and disordered porous plaster
300 structure (in gypsum chemical form). Regarding spatial localization of the two water

populations, the first one (P1) extends uniformly in space while the second one (P2) is more confined and isolated in some clusters of gypsum needles (Jaffel et al. 2006). Distribution of the two populations is related to w/p values and at low w/p value, P2 increased and P1 decreased, in agreement with total porosity observed as a function of water-to-plaster ratio (w/p). Moreover, from a microstructural point of view, an intricated percolation networks of needles with different packing density exists in hardened plaster structure where percolation threshold for allowing water exchange is about w/p=0.6: below w/p= 0.6, there is an extremely slow exchange rate (almost zero) and the two water populations are almost independent. Above w/p=0.7, there is a small but finite exchange rate between the two water populations, however composite permeability was not sufficient to run PRB kinetic studies in short times.

Presence of mineral acids influence gypsum crystallization step, promoting formation of large bulky crystals (Mori 1982). Because of increasing in particle size due to increased growth rate (Al-Othman and Demopoulos 2009), strength of hydrochloric acid-containing samples was increased and their porosity similar to samples in absence of acid (Table 3), However, goal of our research was to increase plaster permeability in order to accelerate degradation reactions and not to ameliorate composite mechanical properties. For these reasons hydrochloric acid was not used in further experiments.

It has to be observed that in the absence of carbonate, porosity was higher with respect to samples in Table 2, indicating that $CaCO_3$ could also act as buffer to stop the acid reactivity and control porosity. However, if porosity of different plaster slabs, as numeric values obtained from sample densities, with and without porogen, was not so different (62% vs 55%, Table 4), permeability was extremely dependent on porogen nature, differing about three orders of magnitude (Table 5).

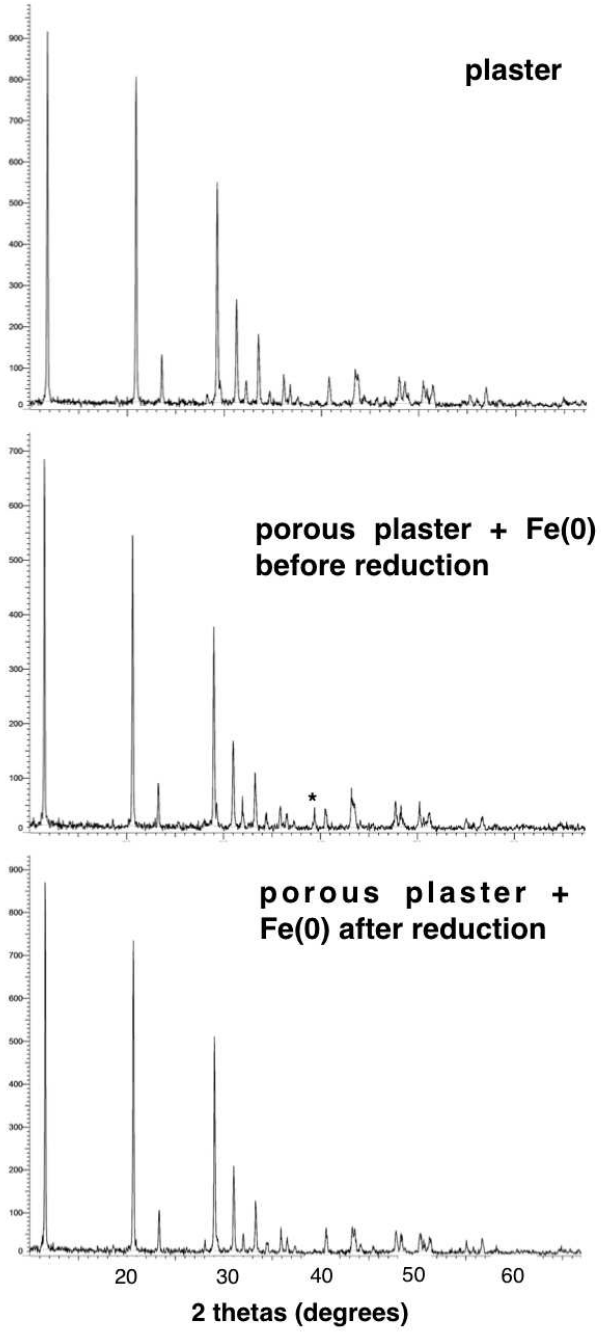

Depending on ZVI amounts (Table 4), density and mechanical properties were increased, porosity was reduced whereas, however permeability remained similar than in absence of ZVI.

3.1.2 Composite characterization

XRD diffractograms for plaster samples (Figure 4) were compatible with those of gypsum (COD 2300259). For composites, porous, with and without ZVI, all chemicals other than calcium sulfate were less than 10% and major deflection angle at 44.8° (2θ) for Fe(0) (Khalil et al. 2018) not detected by XRD. In fact, in these experimental condition, it could be observed, mixed to gypsum, only with 50% Fe(0). However, in composites containing Fe(0) a deflection angle at 39.5° was present but disappeared after PNA reduction (Figure 4) indicating presence of reactive iron species not clearly identified by DRX data.

Figure 4 DRX of plaster composites, with and without Fe(0), before and after PNA reduction. Composites were formulated as in Tables 1 and 4

3.2. Chemical reduction (Bechamp reduction)

3.2.1. ZVI reactivity in batch reduction

In order to identify the best experimental conditions, Bechamp reduction was checked batchwise. Experiments were run as a function of ZVI amount, in absence and in presence of phosphoric acid to activate reduction. "Classical" Bechamp reduction (Béchamp 1854) is run with acetic acid (or hydrochloric acid), which does not form insoluble species after oxidation of ZVI to Fe(II) or Fe(III); in fact possible formation of insoluble iron phosphate was expected in our experimental conditions, however nothing was reported in literature to support its role in Bechamp reduction. As a function of time, yellow solution turned pale: also in absence of acid, reduction occurred and after 7 hours almost no PNA remained in solution (Figure 5).

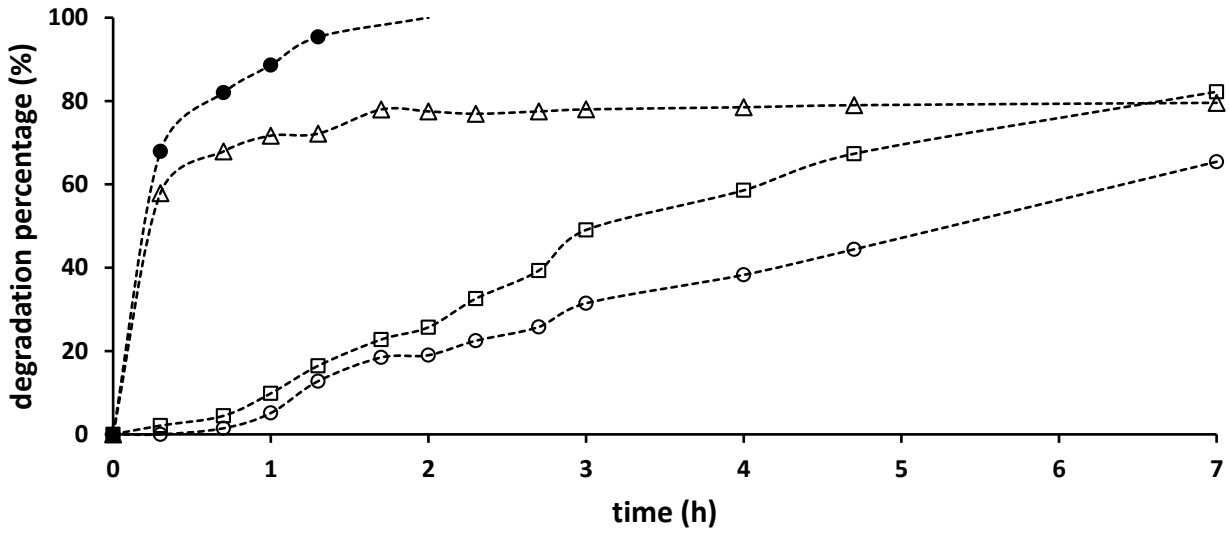

376

377 **Figure 5** Degradation of PNA in Bechamp reduction as a function of time and of ZVI
378 percentage: 1.2 (○); 2.3 (□); 3.4(△); 1.0 % + 1.0 % H_3PO_4(●); [PNA]=30 mg/l

379

380 In presence of H_3PO_4 (0.4%) or higher amount of ZVI (>3%), the reaction was faster and total
381 reduction occurred in 1 hour. Samples recovered after reduction, with or without acid,
382 became violet by standing and solutions were cloudy: the presence in solution of ionic iron
383 species can form insoluble iron hydroxydes (even if at acidic pH, Figure 6) which explained
384 cloudy diffusion. Redox reaction was not halted to PDA and polymerization of aromatic
385 molecules also occurred, as usual in presence of metal ions (Lajoie-Halova et al. 2006;
386 Sapurina and Stejskal 2008). In addition, formation of iron hydroxo species seemed justified
387 because pH values increased at the end of Bechamp reduction, in all experimental conditions
388 (Figure 6).

389

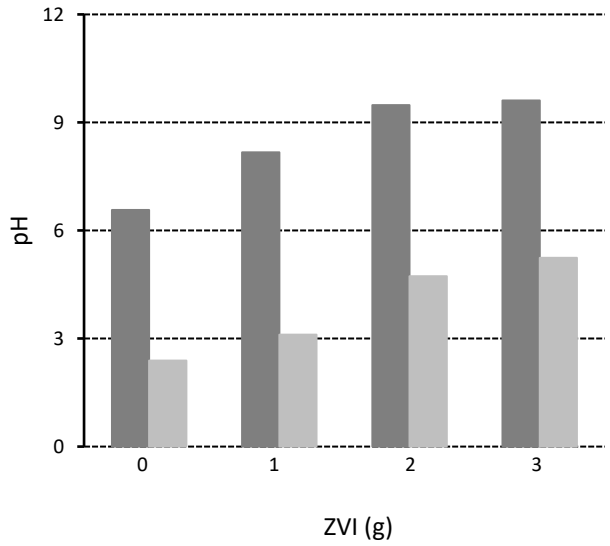

390

391 **Figure 6** Final pH values of solutions in batch Bechamp reduction after 7 hours, as a fonction
392 of ZVI: without acid (dark grey); with 1 % H_3PO_4 (light grey)

393

394 3.2.2. ZVI reactivity in column reduction

395 PNA solutions were added to columns (Fig. 7) and, after percolation, fractions (100 ml) were
396 recovered and analyzed by Vis-UV spectroscopy. In all experiments, yellow colour of PNA
397 solutions disappeared indicating that Bechamp reduction occurred in plaster columns. In
398 order to verify chemical effects in colour fading, UV-Vis spectra were registered between
399 200 and 700 nm: PNA was reduced to PDA indicating that Bechamp reaction occurred in
400 plaster column (Figure 1). As observed in batch experiments, PDA aqueous solutions were
401 not stable as a function of time and pale yellow solutions became hazy and violet colored,
402 indicating polymerization of aromatic amines.

403

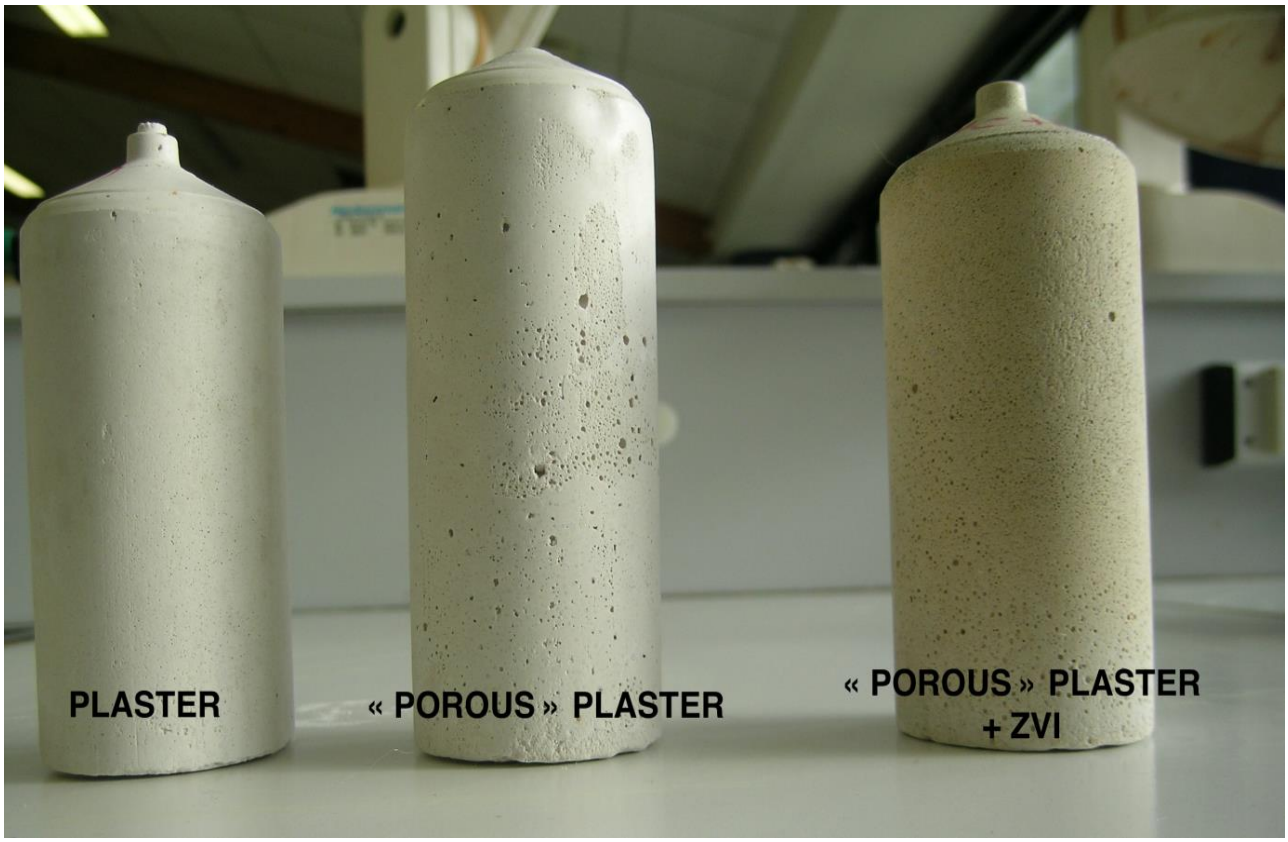

404 **Figure 7** Plaster columns. Column composition: plaster (50.0 g, 41.0%); water (57.4%);
405 $CaCO_3$ (0.2%); H_3PO_4 (1.4%); ZVI (2.3%)

406 Degradation profiles, as a function of time at different concentration of PNA and ZVI, were
407 reported in Figure 8. The flow through the columns was around 0.3 ml/min and increased as a
408 function of added volume at about 25%

409

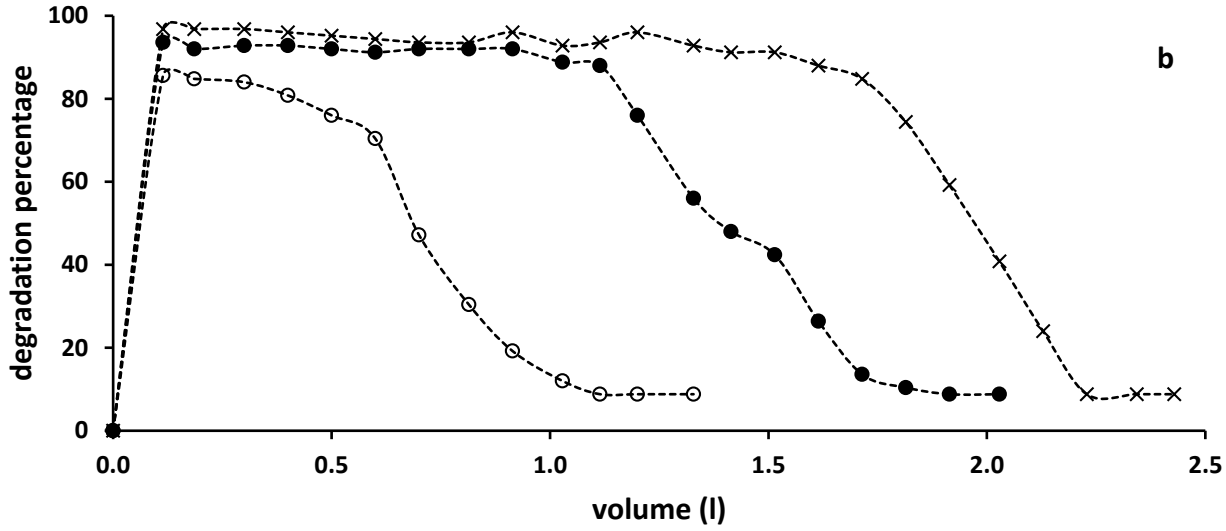

410

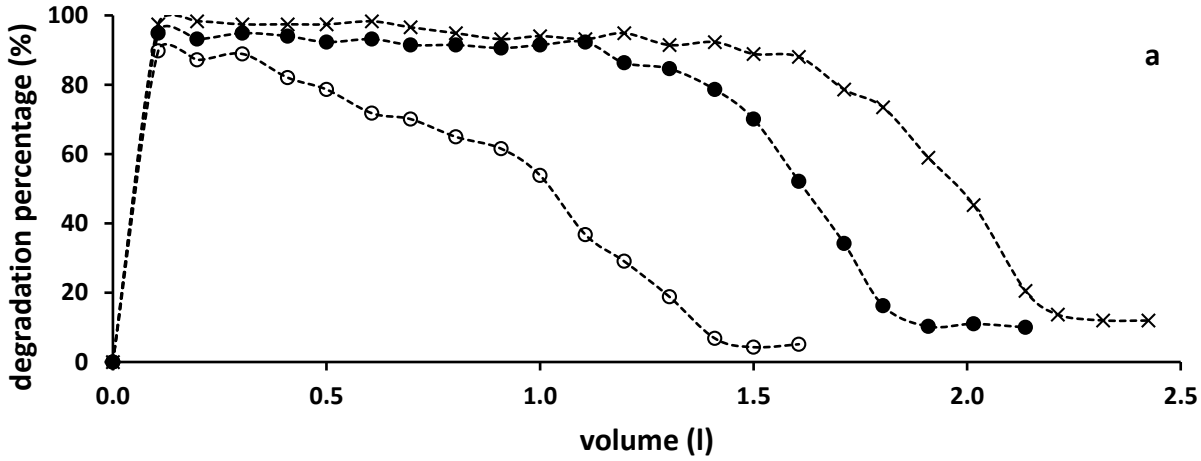

411
412

413 **Figure 8** Degradation profiles of p-nitroaniline as percentage (PNA= 30 mg/L (a), 100 mg/L
414 (b)) as a function of elution volume and ZVI percentage. ZVI: 1.2 (○), 2.3 (●), 3.4 % (x);
415 column composition (without ZVI): plaster (200.0 g, 41.0%); water (57.4%); $CaCO_3$ (0.2%);
416 H_3PO_4 (1.4%)

417 As expected, breakthrough points in Bechamp reduction were depending on ZVI amount
418 included in plaster column; PNA concentration seemed have less influence because
419 degradation profiles in Figure 7 (except those with low quantity of ZVI (1.2%)) were almost
420 superimposable.

From degradation reaction, the amount of PNA reduced to PDA by ZVI (in 2.3 and 3.4% experiments) was estimated: e.g. 1.6 L of aqueous PNA solution at 100 mg/L were treated by 3 g of ZVI, meaning a complete inactivation at around 55 mg of PNA ($3.0 \cdot 10^{-4}$ mol) per gram of ZVI ($1.8 \cdot 10^{-2}$ mol) moles), or around 2×10^{-2} mol PNA per 1 mol Fe(0).

3.2.3 Degradation reaction

In order to indentify mechanism of PNA reduction in plaster columns, oxidation products from ZVI were searched. Unfortunately the low percentage of metal species in plaster composites did not allow to clearly identify by DRX intermediate species in ZVI oxidation process. Moreover, because of coloured solution for PNA and PDA, Fe(II) or Fe(III) species colorimetric identification in solution was not possible. For these reasons, control experiments were run in order to observe chemical species formed by interaction of ZVI with water. For instance, treating ZVI with H_3PO_4, presence of Fe(II) was detected by colorimetry, which seemed confirm the predominance of Fe(II) in Bechamp mechanism (Popat and Padhiyar 2013).

	pH (t=0)	pH (t=48 h)	Fe(II) test	Fe(III) test
Plaster	6.92	6.87	n.d.	n.d.
Plaster + ZVI	6.76	7.45	-	-
Plaster + ZVI + $CaCO_3$+ H_3PO_4	6.91	7.09	+	-

Table 6 pH values and qualitative colorimetric results for ionic iron species in plaster-based composites soaked in distilled water

In ZVI-containing column, during the addition of PNA solutions, the first volume eluted was slightly acid (pH value = 5.22), probably because of presence of acid trace, whereas, as a

443 function of volume of organic species added, solution pH was determined by the presence of
444 specific organic compound (PDA, pH = 8.07; PNA, pH = 6.10 for 30mg/l aqueous solutions)

445 However, because of instability of Fe(II) species in aqueous solution in presence of dioxygen,
446 at the end of the reduction process, reddish colour of column indicated presence of Fe_3O_4
447 species

448 From our experimental results, we cannot exclude or affirme the presence of other iron
449 species such as oxides, hydroxides, or phosphates and make hypothesis on their involvement
450 in reduction reaction.
451

452 3.2.4. Kinetics analysis

453 Bechamp reduction is a stoichiometric reaction, and not a catalytic one, resulting in a series
454 of parallel reactions, with generation of one or more intermediates and byproducts (Popat &
455 Padhiyar, 2013). ZVI is "consumed" in redox system (or, from a chemical point of view,
456 oxidated) and/or, probably, passivated during flow of aqueous solutions. However, it has
457 been reported by Noubactep that, in order to minimize the abundance of iron corrosion
458 products in a ZVI/H_2O system, the following operations can be undertaken: (i) use the lowest
459 possible Fe(0) loading (e.g. <5 g/l); (ii) work under non-disturbed conditions (mixing speed 0
460 min^{-1}) or low mixing conditions; (iii) used a less reactive material; (iv) work at low
461 temperature (e.g. 15°C). (Noubactep 2009). In our case, if the first point was respected, in
462 order to accelerate kinetics time, we used a special porous plaster with a high flow, which
463 could accelerate reducing agent disruption. Of course, in an environmental application, it
464 would be possible to alternate in PRB porous plaster blocks (in order to absorb more polluted
465 solution) and ZVI-containing compact plaster blocks (in order to act as reducing agent).
466 However, Bechman reaction in PRB seems to be more complex than in solution. In fact, if

contaminant reduction by Fe(0) occurs and contributes significantly to the process of contaminant removal, this mechanism remains unclear. In fact, it is matter of question in ZVI depolluting systems, if, between the Fe(II)/Fe(0) or Fe(III)/Fe(II) couples, which one is involved in the redox reactions (Noubactep 2008). From our point of view, we checked in batch direct reaction between ZVI and PNA without acid and the reduction occurred with a kinetics depending on ZVI amount. As a consequence, we expected that Fe(0) would be directly involved in the redox system; however kinetics, in batch and in column were not the same (in column the reaction was instantaneous) suggesting that preliminar treatement with phosphoric acid acted also on ZVI, partially generating Fe(II) species. It means that Fe(II) species could be involved in order to accelerate reduction rate, whereas, it remains the question of Fe(II) species stability (excepted in the form of phosphate salt), which is possible only dried or in the absence of dioxygen.

If phosphoric acid, reacting with ZVI, can form Fe(II) species, more efficient as redox couple, unfortunately nothing is known on the role of iron phosphate in Bechamp reduction. We can speculate on the possibility that in-situ formed ionic species could coordinate organic molecules in order to favor, by molecular proximity, redox reaction. Between Fe(II) or Fe(III) species, the former has preferential affinity to bind nitrogen-containing ligand (Cotton & Wilkinson, 1988). On this half, studies are actually in progress to evaluate how organic chemical structure could influence redox reaction.

Noubactep reported also that corrosion products form an active physical barrier reducing the accessibility of the bare surface of Fe(0) materials to contaminants getting inactivation of ZVI (Noubactep 2007). It has been suggested, for instance, that “solution decoloration” could occur because of concomitant precipitation of iron hydroxydes (Noubactep 2009a), which absorb organic compounds as we previously observed co-precipitation in case of hydroxyapatite (Lemlikchi, et al. 2014.). From our experience, we cannot totally exclude this

492 mechanism (Noubactep 2011), whereas PDA recovering, in the first fractions, strongly
493 suggested that redox mechanism was predominant.
494 We observed that, as a function of time, flow through the column increased by 25%.
495 Different hypothesis can made on the interaction between PNA and ZVI. Concerning the
496 flow, two different mechanisms seemed to occur: on one hand, plaster columns were
497 sensitive to percolation, and, as a function of water volume, were fragilized. On the other, in
498 situ formation of insoluble iron species, such as hydroxides or phosphates, in sol or in gel
499 form, could plug the porosities (Noubactep 2008), but with this hypothesis, the flow would be
500 reduced.
501

502 *3.3. Environmental impact and cost*

503 The cost of plaster-based PRB is estimated to be very low and convenient. PDA, the
504 reduction product of PNA, is a still toxic species, but it could be captured on column with
505 special additives (not reported here).

506 An ideal PRB should present the following advantages:
507 i) chemical reactivity, which is related to reactant contact time, depending on kinetics and
508 flow. Chemical reactivity involves also compatibility between reactive species and barrier
509 materials.
510 ii) stability during PRB lifetime in order to minimize lost of efficiency;
511 iii) hydraulic and mechanical performances: PRB permeability has to be higher than aquifer
512 flow in order to not disturb underground flow and not induce polluted flow out of the barrier.
513 The supporting material should also be shaped in blocks in order to easily build PRB and, of
514 course, with good mechanical properties for barrier stability;

iv) reduced environmental impact in order to not increase pollution effects: PBR has to be mainly constituted by inert and non-toxic materials, producing, when possible, non-toxic and harmless by-products;

v) cost of PRB building (in terms of materials and construction process as low as possible in order to be economically feasable.

Finally, the efficiency of ZVI in plaster based-columns suggest the use of these composite as precast plaster retaining wall blocks in environmental applications.

4. Conclusion

PRB was used to purify water from organic contaminants, such as 4-nitroaniline. Plaster is one of the most used materials in construction industry. It can also be used in PRB, and while it is being made the plaster can incorporate many types of additives. We have included ZVI to make a reactive component with capacity to remove nitro compounds while the water flow passes through the plaster. The use of ZVI as additive in the PRB allows removing the toxic organic compound by reduction of the nitro function to amino functions. To provide a PRB with good flow through properties, the formulation of porous plaster with increased porosity was made possible by the reaction of calcium carbonate with a small amount of phosphoric acid, which causes the evolution of carbon dioxide gas simultaneously with the precipitation of hydroxylapatite effectively making the plaster less water soluble. Thus improved PRB containing plaster, designed porosity and ZVI particles can be developed for use in removal of organic compounds from water. This opens possibilities for the use of PRB in many pollution control technologies where it could be scaled up.

Declarations

Consent for publication

Not applicable

Availability of data and materials

All data generated or analysed during this study are included in this published article

Competing interests

Authors have not financial and non-financial competing interests on this research field

Ethical approval

Not applicable

Consent to participate

Not applicable

Funding

This research did not receive any specific grant from funding agencies in the public, commercial or not-for-profit sectors.

Authors' contributions

MF and PS conceived the study, were in charge of overall direction and planning and were major contributors in writing the manuscript. SB and MF processed experimental data, formulated composites, performed analysis, and drafted the manuscript. FF prepared samples, performed SEM analysis and worked on the manuscript. All authors discussed the results and commented on manuscript.

Acknowledgements

SB is grateful to the Algerian Ministry of Education for the fellowship.

The authors thank dr. Farid Errassifi (ILIPACK, PEC Department, Université Toulouse 3 Paul Sabatier, Castres, France) for technical assistance in the mechanical strength measurements.

Abbreviations used

PDA, p-phenylendiamine; PNA, 4-nitroaniline; PRB, permeable reactive barrier; ZVI, zero valent iron;

REFERENCES

Adrien J, Meille S, Tadier S, Maire E, Sasaki L (2016) In-situ X-ray tomographic monitoring of gypsum plaster setting. Cem Concr Res 82:107–116

Al-Othman A, Demopoulos G.P (2009) Gypsum crystallization and hydrochloric acid regeneration by reaction of calcium chloride solution with sulfuric acid. Hydrometallurgy 96: 95–102

Béchamp A (1854) De l'action des protosels de fer sur la nitronaphtaline et la nitrobenzine. nouvelle méthode de formation des bases organiques artificielles de Zinin. Ann Chim Phys 42:186-196

CRC Handbook of Chemistry and Physics, 2019, 100th Edition, John Rumble ed. CRC Press.

Chernysh Y, Yakhnenko O, Chubur V, Roubik H (2021) Phosphogypsum Recycling: A Review of Environmental Issues, Current Trends and Prospects. Appl. Sci. 11 :1575. https://doi.org/10.3390/app11041575

Cotton F.A, Wilkinson G (1988) Advanced Inorganic Chemistry, John Wiley, New York, pp 709-724

Diaga Seck M, Van Landeghem M. Faure P, Rodts S, Combes R, Cavalie P, Keita E, Coussot P. (2015) The mechanisms of plaster drying. J Mat Sci 50:2491-2501

Dorathi P.J, Kandasamy P (2012) Dechlorination of chlorophenols by zero valent iron impregnated silica. J Environ Sci 24:765–773

Eljamal O, Mokete R, Matsunaga N, Sugihara Y (2018) Chemical pathways of Nanoscale Zero-Valent Iron (NZVI) during its transformation in aqueous solutions. J Environ Chem Eng. 6:6207-6220. https://doi.org/10.1016/j.jece.2018.09.012

Eljamal O, Thompson IP, Maamoun I, Shubair T, Eljamal K, Lueangwattanapong K, Sugihara y (2020) Investigating the design parameters for a permeable reactive barrier consisting of nanoscale zero-valent iron and bimetallic iron/copper for phosphate removal. J Mol Liq 299:112144. https://doi.org/10.1016/j.molliq.2019.112144

Farooqi ZH, Khalid R, Begum R, Farooq U, Wu Q, Wu W, Ajmal M, Irfan A, Naseem K (2018) Facile synthesis of silver nanoparticles in a crosslinked polymeric system by in situ reduction method for catalytic reduction of 4-nitroaniline. Environ Technol 40:1-30

Fisher RD, Hanna JV, Reesc GJ, Walton RI (2012) Calcium sulfate-phosphate composites with enhanced water resistance. J Mater Chem 22:4837-4846

605 Gavrilescu M, Demnerová K, Aamand J, Agathos S, Fava F (2015) Emerging pollutants in
606 the environment: present and future challenges in biomonitoring, ecological risks and
607 bioremediation. New Biotechnol 32:147-156
608 Grajales-Mesa S.J, Malina G (2016) Screening reactive materials for a permeable barrier to
609 treat TCE-contaminated groundwater: laboratory studies. Environ Earth Sci 75:772-
610 785.
611 Henderson AD. Demond AH (2007) Long-Term Performance of Zero-Valent Iron Permeable
612 Reactive Barriers: A Critical Review. Environ Eng Sci 24:401-423
613 Hu R, Cui X, Willis Gwenzi W, Wu S, Noubactep C (2018) Fe0/H_2O Systems for
614 Environmental Remediation: The Scientific History and Future Research Directions.
615 Water SA 10:1739-1755. https://doi:10.3390/w10121739
616 Jaffel H, Jean-Pierre Korb JP, Ndobo-Epoy JP, Morin V, Guicquero JP (2006) Probing
617 Microstructure Evolution during the Hardening of Gypsum by Proton NMR
618 Relaxometry. J. Phys. Chem. B 110: 7385-7391
619 Khalil AME, Eljamal O, Amen TWM, Sugihara Y, Matsunaga N (2018) Scrutiny of
620 interference effect of ions and organic matters on water treatment using supported
621 nanoscale zero-valent iron. Environ Earth Sci (2018) 77:489.
622 https://doi.org/10.1007/s12665-018-7661-6
623 Lajoie-Halova B, Brumas V, Fiallo MML, Berthon G. Copper(II) interactions with non-
624 steroidal anti-inflammatory agents. III – 3-Methoxyanthranilic acid as a potential OH-
625 inactivating ligand: A quantitative investigation of its copper handling role in vivo. J
626 Inorg Biochem (2006) 100:362. https://doi:10.1016/j.jinorgbio.2005.12.002
627 Lanzóna M, García-Ruiz PA, 2012. Effect of citric acid on setting inhibition and mechanical
628 properties of gypsum building plasters. Constr Build Mater 28:506-511

629 Lemlikchi, W, Sharrock P, Fiallo M, Nzihou A, Mecherri MO (2014) Hydroxyapatite and
630 Alizarin sulfonate ARS modeling interactions for textile dyes removal from
631 wastewaters. Procedia Eng 83:378-385
632 Lewry A.J, Williamson J (1994) The setting of gypsum plaster: part I. The hydration of
633 calcium sulphate hemihydrate, J Mater Sci 29:5279–5284
634 Maamoun I, Eljamal O, Khalil AME, Sugihara1 Y, Matsunaga N (2018) Phosphate
635 Removal Through Nano-Zero-Valent Iron Permeable Reactive Barrier; Column
636 Experiment and Reactive Solute Transport Modeling. Transport in Porous Media
637 125:1-3. https://doi.org/10.1007/s11242-018-1 124-0
638 Maamoun I, Eljamal O, Eljamal R, Falyouna O, Sugihara Y (2020) Promoting aqueous
639 and transport characteristics of highly reactive nanoscale zero valent iron via
640 different layered hydroxide coatings App Surf Sci 506 :145018.
641 https://doi.org/10.1016/j.apsusc.2019.145018
642 Maamoun I, Eljamal O, Omar Falyouna, Eljamal R, SugiharaY (2020a) Multi-objective
643 optimization of permeable reactive barrier design for Cr(VI) removal from
644 groundwater Ecotoxicol Environ Saf 200:110773.
645 https://doi.org/10.1016/j.ecoenv.2020.110773
646 Mori T (1982) The Effect of Boric Acid on the Thermal Behavior of Cast Gypsum. Dental
647 Materials Journal 1:73-80
648 Noubactep C (2007) Processes of Contaminant Removal in "Fe0-H_2O" Systems Revisited:
649 The Importance of Co-Precipitation Open Environ J. 1:9-13
650 Noubactep C (2008) A Critical Review on the Process of Contaminant Removal in Fe0–H_2O
651 Systems Environ Technol 29:909-920
652 Noubactep C (2009) An analysis of the evolution of reactive species in Fe0/H_2O systems. J
653 Hazard Mat 168:1626–1631

654 Noubactep C (2009a) Characterizing the discoloration of methylene blue in Fe0/H_2O systems.
655 J Haz Mat 166:79–87
656 Noubactep C (2011) Aqueous contaminant removal by metallic iron: Is the paradigm
657 shifting? Water SA 37:419-426
658 Popat V, Padhiyar N (2013) Kinetic Study of Bechamp Process for P-Nitrotoluene Reduction
659 to P-Toluidine. Int J Chem Engineer Appl. 4:401-405
660 Saadaoui E, Ghazela N, Ben Romdhanea C, Massoudi N (2017) Phosphogypsum: potential
661 uses and problems - a review. Int J Environ Stud 74(4):558-567.
662 http://dx.doi.org/10.1080/00207233.2017.1330582
663 Sapurina I, Stejskal J (2008) The mechanism of the oxidative polymerization of aniline and
664 the formation of supramolecular polyaniline structures. Polym Int 57:1295–1325
665 Schabel T, Belger C, Plietker B (2013) A Mild Chemoselective Ru-Catalyzed Reduction of
666 Alkynes, Ketones, and Nitro Compounds. Org Lett 15 :2858-2861
667 Touze S, Chartier R, Gaboriau H (2004) Etat de l'art sur les barrières perméables réactives
668 (BPR): Réalisations, expériences, critères décisionnels et perspectives; BRGM Orléans,
669 France. www.record-net.org/storage/etudes/02-0330-1A/rapport/Rapport_record02-
670 0330_1A.pdf
671 Various authors, 1989. Some nitroarenes. In Diesel and Gasoline Engine Exhausts and Some
672 Nitroarenes. IARC Monograph, vol. 46, IARC Lyon, pp. 188-374;
673 monographs.iarc.fr/iarc-monographs-on-the-evaluation-of-carcinogenic-risks-to-
674 humans-75/
675 Various authors, 1989a. Chloramphenicol. In Pharmaceutical Drugs. IARC Monograph, vol.
676 50, IARC Lyon, pp. 169-194; monographs.iarc.fr/iarc-monographs-on-the-evaluation-
677 of-carcinogenic-risks-to-humans-71/
678 Various authors, 1992. Hair Dyes. In Occupation al Exposures of Hairdressers and
679 Barbersand Personal Use of Hair Colourants; Some Hair Dyes, Cosmetic Colourants,

680 Industrial Dyestuffs and Aromatic Amines. IARC Monograph, vol. 57, IARC Lyon, pp.
681 43-118; monographs.iarc.fr/iarc-monographs-on-the-evaluation-of-carcinogenic-risks-
682 to-humans-64/
683 Wantanaphong J, Mooney SJ, Bailey EH (2006) Quantification of pore clogging
684 characteristics in potential permeable reactive barrier (PRB) substrates using image
685 analysis. J Contaminant Hydrol 8:299-320

Figures

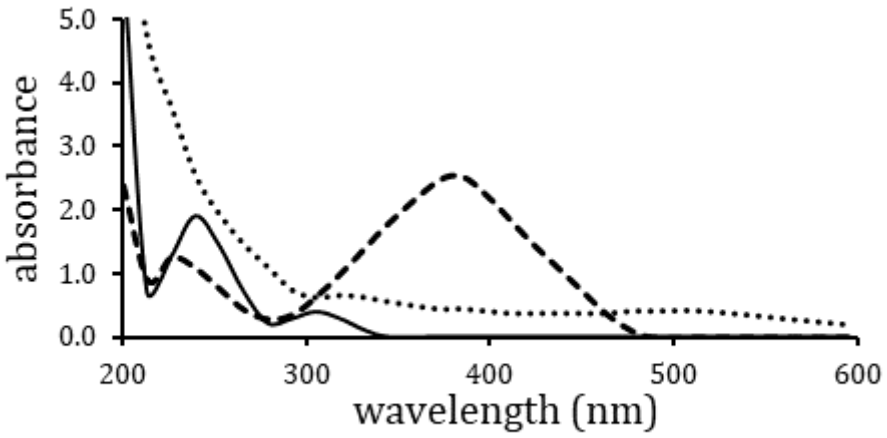

Figure 1

Absorption spectra of PNA (–), PDA (___) and PDA polymerization product (…) in aqueous solutions: [PNA]= [PDA]= 30 mg/l; path-length quartz cell = 0.2 cm

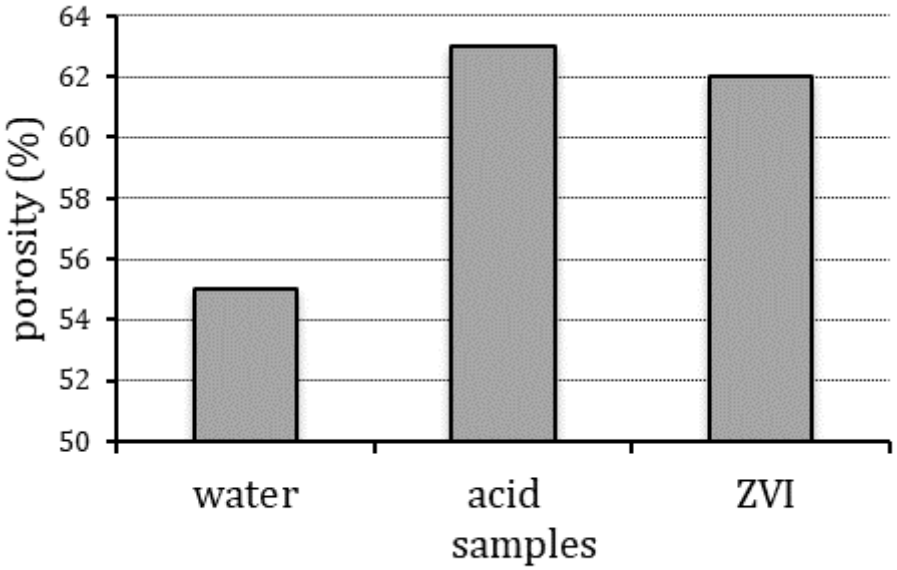

Figure 2

Porosity optimization as a function of different components of BRP (water, phosphoric acid and ZVI) plaster (50.0 g, 40.0%); water (56.0%); CaCO3 (0.2%); H3PO4 (0.2%) Plaster samples were observed by scanning electron microscopy (SEM) Zeiss Supra 55VP.

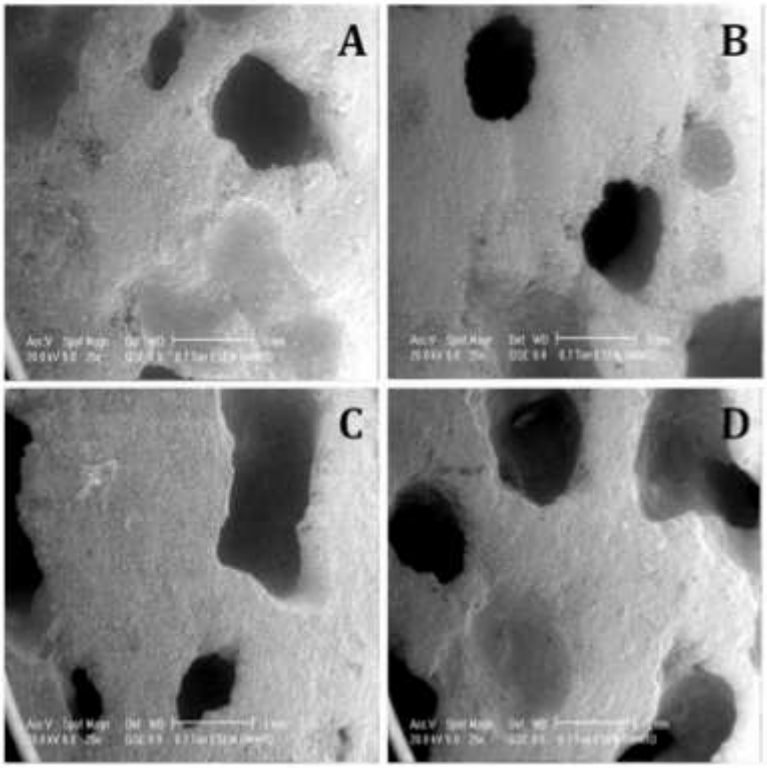

Figure 3

SEM photographs showing a view of porogen-containing hardened gypsum samples, prepared with a water-to-plaster ratio of 0.7, as a function of carbonate amounts (with 1.1 % phosphoric acid, w/w). CaCO3: A=0.2%, B=0.5g, C=0.7g, D= 0.9% (w/w); length scale bar is 1mm and magnification x25)

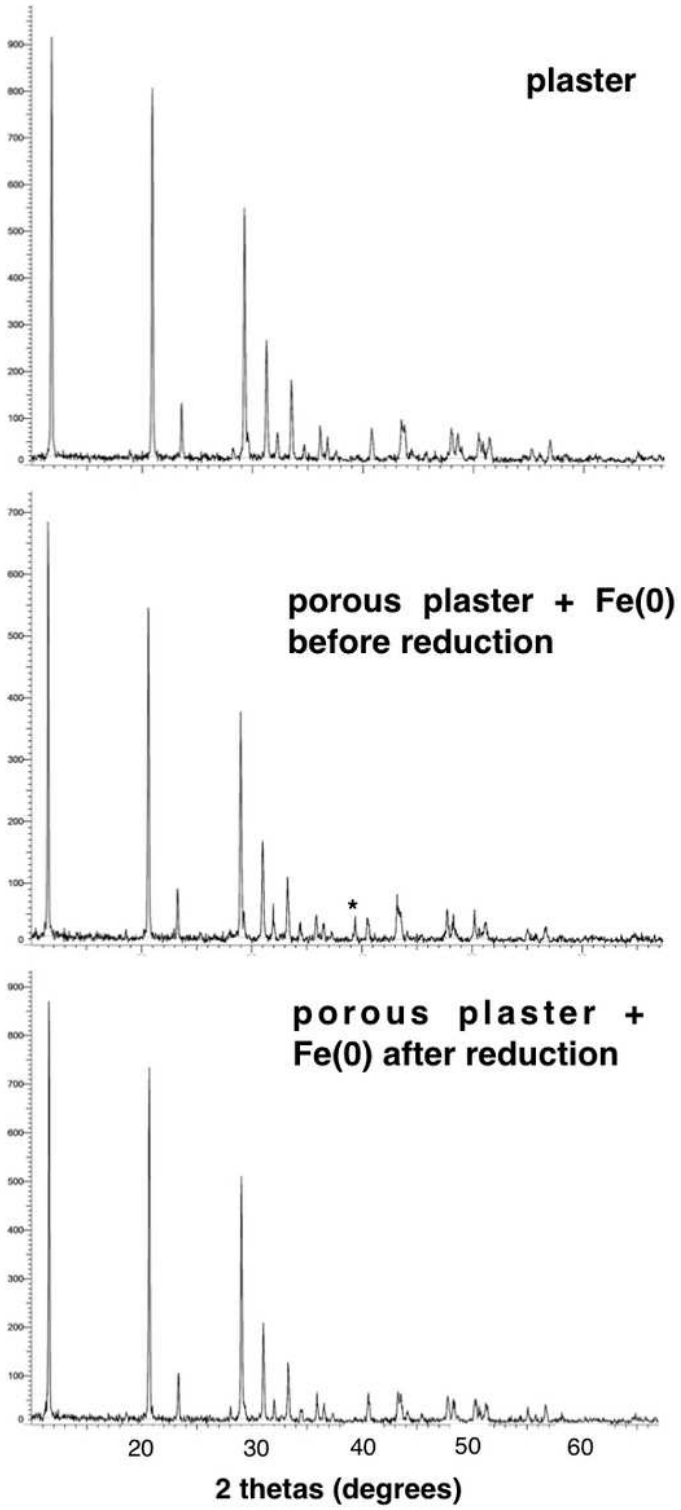

Figure 4

DRX of plaster composites, with and without Fe(0), before and after PNA reduction. Composites were formulated as in Tables 1 and 4

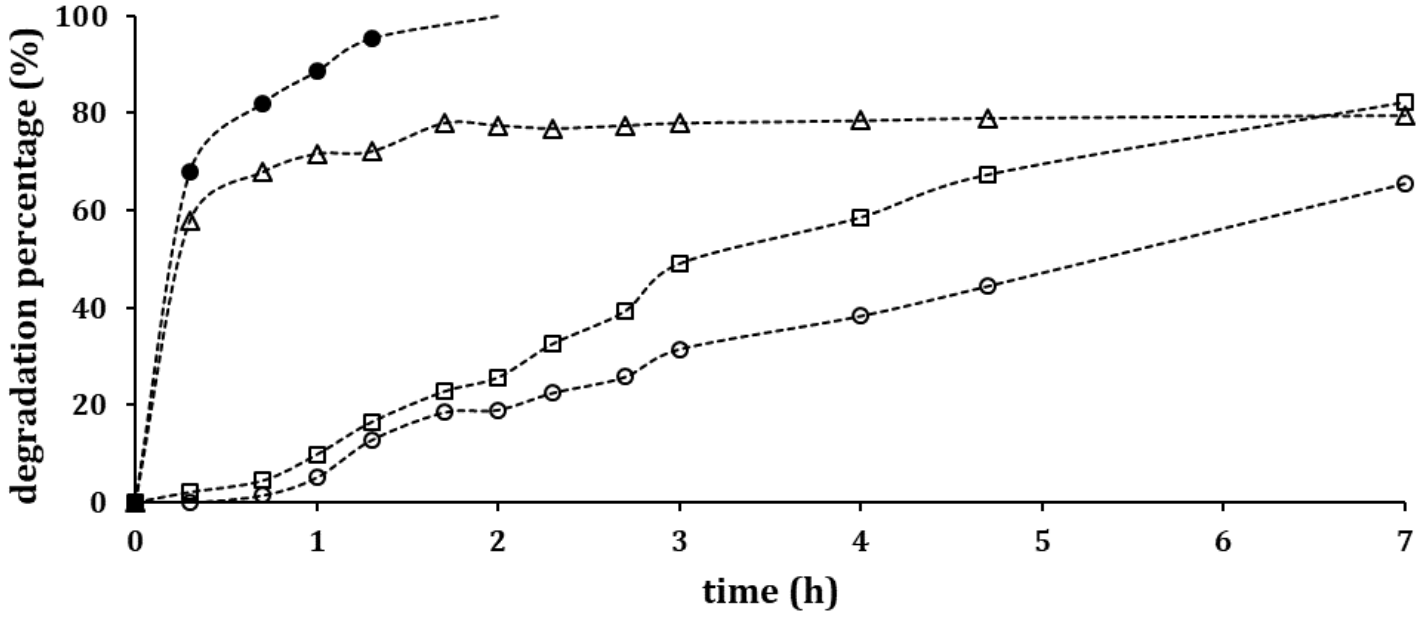

Figure 5

Degradation of PNA in Bechamp reduction as a function of time and of ZVI percentage: 1.2 (□); 2.3 (□); 3.4(□); 1.0 % + 1.0 % H3PO4(□); [PNA]=30 mg/l

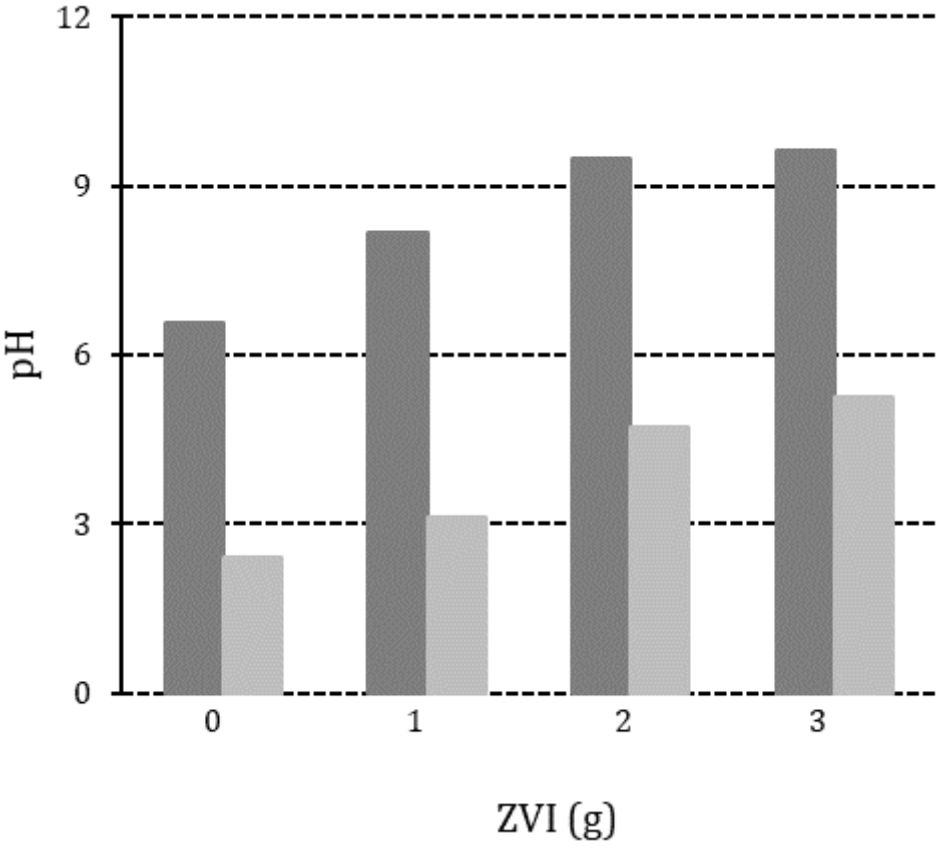

Figure 6

Final pH values of solutions in batch Bechamp reduction after 7 hours, as a fonction of ZVI: without acid (dark grey); with 1 % H3PO4 (light grey)

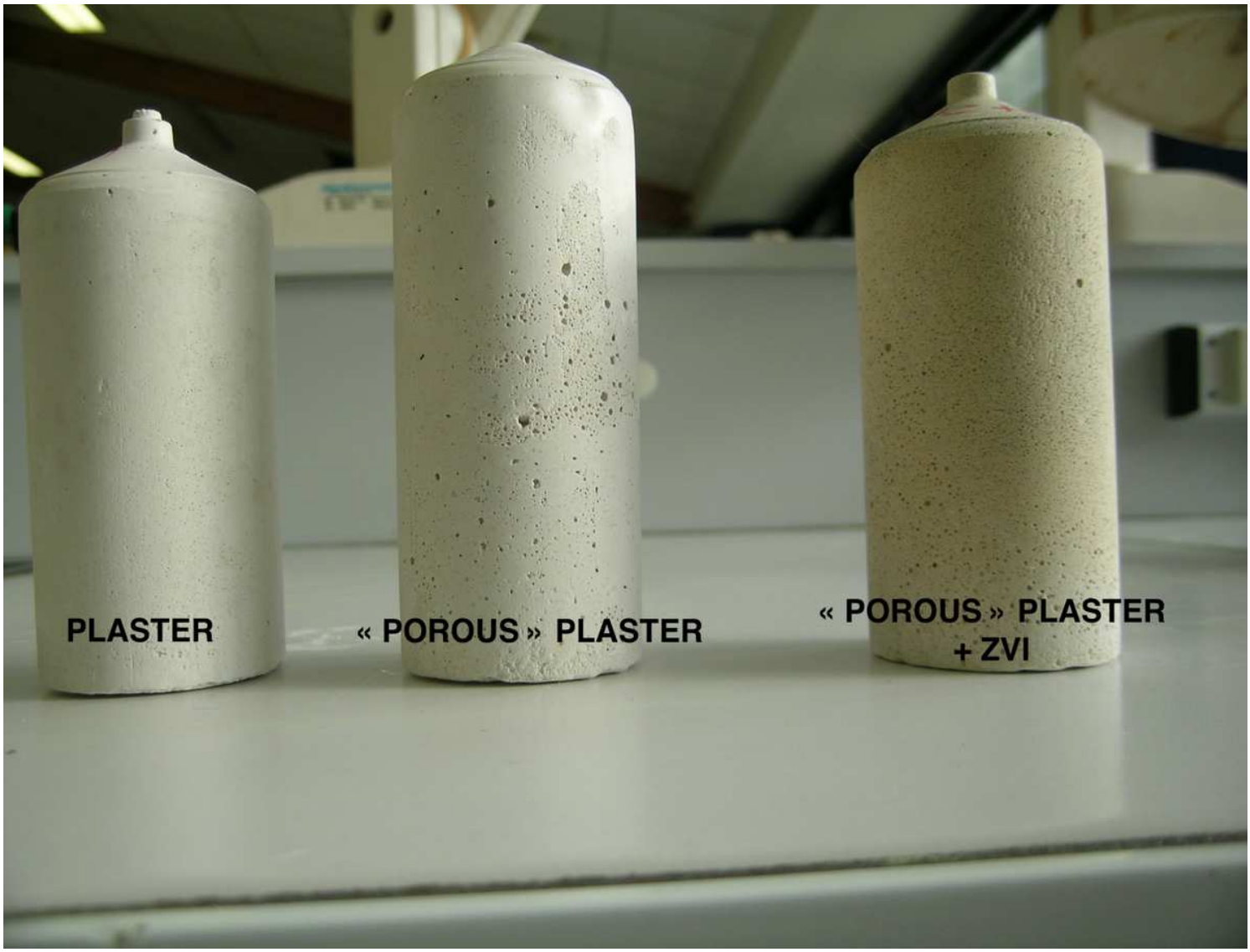

Figure 7

Plaster columns. Column composition: plaster (50.0 g, 41.0%); water (57.4%); CaCO3 (0.2%); H3PO4 (1.4%); ZVI (2.3%)

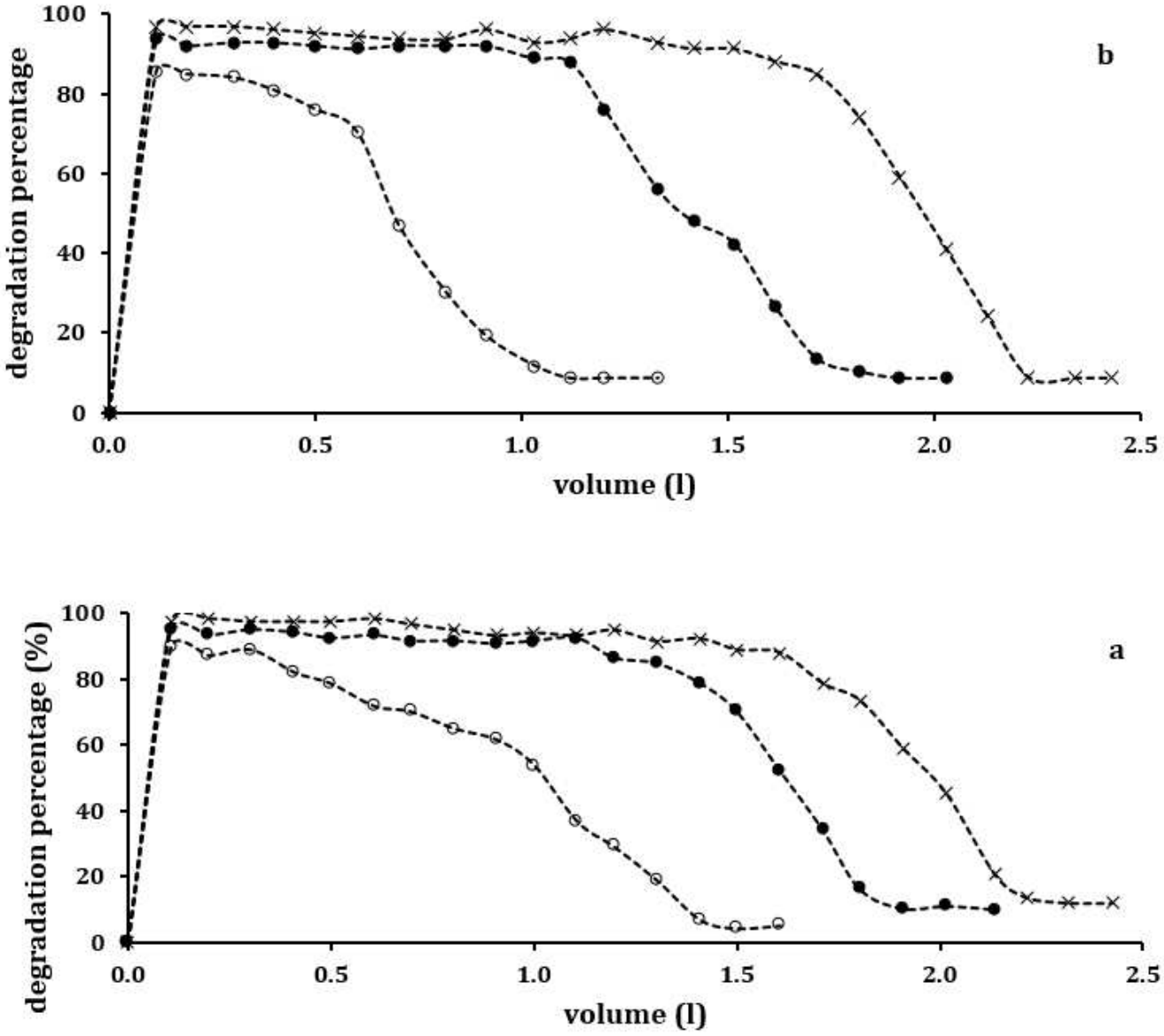

Figure 8

Degradation profiles of p-nitroaniline as percentage (PNA= 30 mg/L (a), 100 mg/L (b)) as a function of elution volume and ZVI percentage. ZVI: 1.2 (□), 2.3 (□), 3.4 % (x); column composition (without ZVI): plaster (200.0 g, 41.0%); water (57.4%); CaCO3 (0.2%); H3PO4 (1.4%)

Supplementary Files

This is a list of supplementary files associated with this preprint. Click to download.

- GraphicalAbstract.jpg